



EUROPEAN SOUTHERN OBSERVATORY

Organisation Européenne pour des Recherches Astronomiques dans l'Hémisphère Austral

Europäische Organisation für astronomische Forschung in der südlichen Hemisphäre

LA SILLA OBSERVATORY

┌ Science Operations ┐

└ CES Users Manual ┘

Doc. No. 3P6-MAN-ESO-90100-0004

Issue 1.0

Date 03/10/2004

┌ ┐
Keywords: CES, Users Manual, Spectroscopy, High Resolution

Prepared T. H. Dall 03/10/2004
Name Date Signature

Approved T. H. Dall 03/10/2004
Name Date Signature

Released E. Pompei dd/mm/yyyy
Name Date Signature

This page was intentionally left blank

Change Record

| Issue/Rev. | Date | Section affected | Reason/Initiation/Documents/Remarks |
|------------|----------------------------------|------------------|---|
| 1.0 | Sep 2004 Jun 2004 May 2001 | All All | Now under configuration control. Updating after HCFA integration. Creation. (M.Kürster) |

This page was intentionally left blank

Contents

| | | |
|----------|--|-----------|
| 1 | Introduction | 1 |
| 1.1 | Purpose | 1 |
| 1.2 | Scope | 1 |
| 1.3 | Reference documents | 1 |
| 1.4 | Abbreviations and acronyms | 1 |
| 1.5 | Stylistic conventions | 1 |
| 2 | Overview | 2 |
| 3 | Observing at the 3.6m telescope with CES | 3 |
| 3.1 | Object acquisition | 3 |
| 3.2 | Autoguiding | 4 |
| 3.3 | The quick-look pipeline | 4 |
| 3.4 | Calibrations | 5 |
| 4 | Instrumental characteristics | 7 |
| 4.1 | General description of the CES | 7 |
| 4.2 | Instrument paths | 7 |
| 4.3 | The spectral format of the CES | 7 |
| 4.4 | Achievable resolving power | 7 |
| 4.5 | The image slicer profile | 8 |
| 4.6 | The instrumental efficiency | 9 |
| 4.7 | Signal-to-noise ratios and exposure times | 9 |
| 4.8 | The CES exposure meter | 12 |
| 4.9 | Instrumental stability | 12 |
| 5 | Detector characteristics | 14 |
| 5.1 | General description of CCD #61 | 14 |
| 5.2 | CCD format | 14 |
| 5.3 | CCD read-out speeds and binning | 14 |
| 5.4 | CCD quantum efficiency | 14 |
| 5.5 | CCD cosmetics | 14 |
| 5.6 | Cosmic ray hit rate | 15 |
| 5.7 | Detector monitoring | 15 |
| 6 | The CES observing templates | 17 |
| 6.1 | Genuine Calibration templates | 17 |
| 6.2 | Special Calibration template for wavelength setting | 18 |
| 6.3 | Science template | 18 |
| 6.4 | Acquisition template | 18 |
| 7 | Characteristics of instrument setup delivered to the observer | 20 |
| 7.1 | Alignment of the spectrum with CCD columns | 20 |
| 7.2 | Spectral line tilt | 20 |
| 7.3 | Variation of the width of spectral lines along the slicer profile | 20 |
| 7.4 | Instrument focus | 20 |
| 7.5 | Spectral line width and resolving power | 20 |
| 7.6 | Presence and location of ghost features | 20 |

| | |
|--|-----------|
| 8 Instrument features to be considered for proper data analysis | 21 |
| 8.1 Bias instability | 21 |
| 8.2 Dark current | 21 |
| 8.3 Parasitic light | 21 |
| 8.4 Flatfielding performance | 21 |
| 8.5 Ghost features | 22 |
| 8.6 Treatment of cosmic rays | 22 |
| 8.7 Straylight pedestal | 23 |
| 8.8 Interference pattern seen in continuum | 24 |
| 8.9 An example showing several instrumental features | 24 |

1 Introduction

1.1 Purpose

1.2 Scope

1.3 Reference documents

The following documents are referenced in this document:

[1] The CES web pages: <http://www.lis.eso.org/lasilla/sciops/3p6/ces/>

[2] The P2PP web pages: <http://www.eso.org/observing/p2pp/>

1.4 Abbreviations and acronyms

The following abbreviations and acronyms are used in this document:

| | |
|-------|--|
| CALOB | Calibration OB |
| CES | Coudé Echelle Spectrometer |
| ESO | European Southern Observatory |
| HCFA | HARPS & CES Fiber Adapter |
| HCU | HARPS Calibration Unit |
| HARPS | High Accuracy Radial-velocity Planetary Searcher |
| LSO | La Silla Observatory |
| OB | Observing Block |
| p2pp | Phase 2 Proposal Preparation |
| SA | Support Astronomer |
| SciOp | Science Operations |
| SCS | Standard Calibration Set |
| TIO | Telescope & Instrument Operator |
| VLT | Very Large Telescope |

1.5 Stylistic conventions

Bold and *italic* are used to highlight words. `Teletype` is used for parameters of programs and of p2pp where they appear in the text.

2 Overview

The ESO Coude Echelle Spectrometer (CES) is ESO's highest resolution spectrograph achieving a resolving power of $R = 220,000 - 235,000$. In comparison the maximum resolving power achievable with other ESO spectrographs are $R = 120,000$ for UVES, $R = 100,000$ for HARPS, $R = 70,000$ for EMMI, and $R = 48,000$ for FEROS. The CES is fed via a fibre link to the Cassegrain focus of the 3.6m telescope.

The ESO 3.6m telescope and the CES instrument are operated under ESO's VLT standard. Both the telescope and the instrument are exclusively operated by a telescope-instrument operator (TIO) or by the support astronomer (SA). The TIO carries out so-called observing blocks (OBs) for science observations and calibrations prepared by the visiting astronomer (VA) with the p2pp software [2].

The VA receives an introduction to p2pp by the SA the day before the observing run starts and then prepares the OBs for the program.

During the observations the VA uses a p2pp window to define (and modify, if required) the OBs to be carried out and has access to the obtained data in order to perform quality checks, quick reduction, etc. Moreover, a quick-look reduction pipeline is also available for visual inspection of the data in real-time.

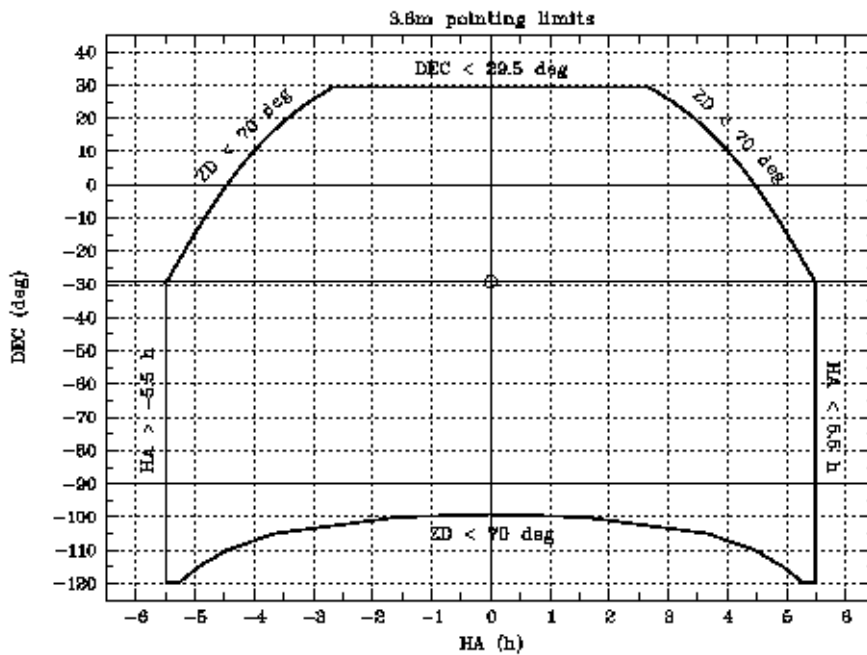


Figure 1: The accessible sky areas of the 3.6m telescope

3 Observing at the 3.6m telescope with CES

The ESO 3.6m telescope in La Silla has an equatorial mount in a horseshoe fork. Instruments are mounted only in Cassegrain focus with a focal ratio of $f/8.09$ for all instruments except TIMMI2 ($f/35$). Diameters of primary mirror, $f/8.09$ secondary mirror and Cassegrain hole are 3566 mm, 1200 mm, and 698 mm, respectively. The clear area of the primary mirror is 88564.3 cm² for the $f/8.09$ secondary. In this mode the image scale in the plane of the Cassegrain focus is 7.02 arcsec/mm.

The sky area accessible to the 3.6m+CES telescope-instrument configuration characterized by the conditions:

- 1 limit in hour angle HA: $-5 \text{ h } 30 \text{ m} < \text{HA} < 5 \text{ h } 30 \text{ m}$
- 2 limit in zenith distance ZD: $\text{ZD} < 70^\circ$
- 3 limit in declination DEC: $-120^\circ < \text{DEC} < +29.5^\circ$

In condition (3) declinations less than -90° refer to an accessible sky region "below" the southern pole, i.e. 12 h away in hour angle with respect to condition (1). Fig. 1 shows a plot of the limits of the accessible sky area (bold line) as a function of hour angle and declination. Note again that also in this figure declinations less than -90° refer to hour angles increased by 12h with respect to the values on the abscissa.

Observers are reminded to account for telescope tracking during the time of the exposure when selecting targets. An overhead of up to 1 min for CCD read-out and data transfer (for normal R/O mode and unbinned CCD) must also be considered (see Tab. 4 in Sect. 5.3).

3.1 Object acquisition

Object acquisition is done using the so-called "slit viewer" camera (a standard VLT denomination) which for the CES fibre link would better be called "fibre viewer". This camera has a technical CCD

and views the field reflected off an inclined plane mirror on top of the fibre head. Currently achieved pointing errors of 5 arcsec rms ensure that the science target ends up well inside the field of view of the technical CCD of this camera ($2.1' \times 2.1'$).

The telescope operator centers the target "manually" (using the telescope control system, TCS) on the fibre hole (a hole in the mirror on top of the fibre head). The focus of the slit viewer camera is usually made in the afternoon and monitored and corrected by the operator during the night.

3.2 Autoguiding

In the standard guiding mode using the slit viewer (fibre viewer) autoguiding is started by the TIO after object centering on the fibre hole. Autoguiding uses a robust center-of-weight algorithm which works on the fraction of object light that does not enter the fibre, but is reflected off the mirror on top of the fibre head. Both the star and fibre positions are continuously computed and updated. With a diameter of the fibre hole of $2''$ on the sky only the wings of the point spread function are employed for the guiding which nevertheless performs well for objects between 2 mag and 16 mag. For brighter objects the telescope operator can insert a filter from the TCS and thus achieve guiding on 0 mag objects.

Typical guiding corrections are $< 0.05''$ rms per coordinate as measured over time scales of 30 min for a 5 - 6 mag star. Corrections are performed with a frequency that can be adapted to the brightness of the object.

For visual binaries the telescope operator can make the size of the guide box smaller (i.e. the region over which the image of the object on the fibre hole is evaluated) in order to avoid light from the companion star to compromise the guiding.

If objects are extended or very close visual binaries (less than $4''$ separation) or if they are too faint for the standard guiding strategy (intrinsically faint or when observing through clouds) then another method must be used. In this case guiding can be performed on the guide probe which is an independent camera with its own technical CCD which can be moved in the telescope focal plane in order to search for a suitable guide star. Note that no automatic guide star search has been implemented for this situation, i.e. when slit viewer and guide probe are simultaneously used. The telescope operator will search for a guide star by moving the guide probe. In this mode target acquisition is done in the manner described above, but the guide probe is used to guide on another star. This is of course less accurate than guiding directly on the fibre.

CES observers should check in advance their target fields for the presence of close companions or extended emission and inform the telescope operator accordingly in order to prepare the best guiding strategy.

3.3 The quick-look pipeline

The CES quick-look tool is exactly that: a quick way to check the quality of the data. It is a background task running on the offline data reduction terminal so the data are automatically reduced and displayed in real time. The program will perform a rough bias subtraction and a linear wavelength fit before displaying the resulting spectrum in units of S/N, providing an immediate measure of the data quality.

For each pixel in the dispersion direction more than 300 pixels are summed across the dispersion, hence cosmic rays are a real problem (see Sect. 8.6). The program removes cosmics with a simple MIDAS routine before extracting the spectrum. The spectra are not flat fielded by default, which is a conscious choice: several spectral orders are contaminated by grating ghosts, which even a simple flatfielding often can remove quite well (see Sect. 8.5). But for checking the data quality, it is

important to be able to see that the ghost is not on top of an important spectral feature, hence we choose to leave out the flat fielding. It can however be turned on at any time without stopping the pipeline.

Observers should be fully aware that the quick-look tool does not provide science quality reductions, but as a means of checking the data quality it does an excellent job.

3.4 Calibrations

The calibration unit used for the CES is the same as used for HARPS, since both instruments have their fibers mounted in the same cassegrain adapter (the HCFA). The calibration unit (the HCU) is located in the HARPS room at the Coudé floor of the 3.6m telescope, from where the calibration light is led to the HCFA via a fibre and via a mirror into the CES fibre. Only two calibration lamps are selectable, a ThAr lamp for wavelength calibration and a Quartz lamp for flatfielding. When taking calibrations the sky field can not be seen in the slit (fibre) view camera.

As of March 2004, new procedures have been implemented for daily calibrations with CES, so that it is no longer up to the VA to take care of his own calibrations, instead SciOps will have to provide standard afternoon and morning calibrations. Some of the daily calibrations will be used for monitoring purposes, but the primary objective is to provide to the VA sufficient high-quality calibrations.

The calibrations foreseen for normal operation of the CES are the following:

- Standard Calibration Set (SCS) taken in the afternoon.
- Solar spectrum just before sunset
- ThAr exposures during the night to ensure accurate wavelength calibration (optional)
- Flat exposures during the night to ensure accurate flatfielding (optional)
- Morning Calibration Set (MCS) generated by CALOB

The optional ThAr and flats during the night are exclusively the responsibility of the VA, as are any spectrophotometric standard star observations. However, for the standards there are predefined OB's available at the telescope for the convenience of the VA.

Under normal operation with only one setup used during the night, the SCS and the MSC are almost identical, containing the calibration frames as detailed in Tab. 1.

Further information on the CES Calibration Plan and CALOB can be found on the CES web pages [1].

Table 1: Standard Calibration Set (SCS) and Morning Calibration Set (MCS) for CES.

| Definition of a SCS | | |
|---------------------|------------------|---------------|
| Type of calibration | Number of frames | exp. time [s] |
| Bias | 7 | 0 |
| Dark | 1 | 1800 |
| Back | 1 | 1800 |
| Flats | 7 | ** |
| ThAr | 1 | ** |
| Solar Spectrum | 2 | ** |

** depends on detector configuration and light path

| Definition of MCS (CALOB) | | | |
|---------------------------|--------|----------------|-----------------------|
| calibration | number | configurations | conditions |
| Bias | 5 | all | |
| Dark | 3 | all | longest exp > 899 sec |
| Back | 1 | all | longest exp > 899 sec |
| Flat | 5 | last | |
| ThAr | 1 | last | |

all = all used detector configurations
last = only the setup (wavelength) left at the end of night

4 Instrumental characteristics

4.1 General description of the CES

The ESO Coude Echelle Spectrometer (CES) is ESO's highest resolution spectrograph achieving a resolving power of $R = 220,000 - 235,000$. It is fed via a fibre link to the Cassegrain focus of the 3.6m telescope. It receives light from the telescope via a single optical fibre on whose entrance in the focal plane the scientific target is centered. The diameter of this fibre on the sky is $2''$. No additional fibre for sky subtraction is available, but for very high resolution spectroscopy of relatively bright targets (> 11 mag) sky subtraction is usually unimportant.

In order to achieve high resolving power an image slicer (of the modified Bowen-Walraven type) is used. The f/12 Very Long Camera (VLC), commissioned in April 1998, provides the required magnification and sufficient sampling of the instrumental profile at this high resolution.

The CES grating is a 79 grooves/mm Echelle in Czerny-Turner mounting. Orders are selected via a prismatic predisperser and only (a part of) one order can be recorded at a time on the CCD.

4.2 Instrument paths

The CES can be used in the 346-1028 nm range (see section 2.6 for the instrument efficiency over this range). In order to optimize efficiency over the whole range, two instrument paths can be selected:

- The BLUE PATH is used at wavelengths below 5025.7 Å
- The RED PATH is used at wavelengths above 5025.7 Å

Observers should note that path changes during the night are not regularly offered. Only in very exceptional circumstances will an effort be made to support them. Path changes will lead to a substantial loss of resolving power (up to a factor 2) due to spectral line tilt (see Sect. 7.3) and loss of instrument focus (see Sect. 7.4). Realignment of the instrument with the goal to eliminate these effects typically takes 2 h or more and is therefore not offered during the night.

4.3 The spectral format of the CES

As only part of a single Echelle order is recorded at a given time on the CCD the spectral bandwidth of the CES is quite limited. It ranges from 22.9 Å in the far blue to 67.7 Å in the far red region of the wavelength regime observable with the CES. Table 2 lists the spectral bandwidth (fifth column) at the blaze wavelengths (third column) for each order (first column). Also listed are the limiting wavelengths for each order (second and fourth column labelled "Min" and "Max"). At the limiting wavelengths the instrumental efficiency drops down to 50% with respect to blaze maximum.

4.4 Achievable resolving power

To achieve the very high resolution, the CES is used with an image slicer instead of a slit. The image slicer slices up the spot of light from the fibre and rearranges the slices in a slit-like fashion. As this "slit" is composed of various slices it has a varying intensity profile (along the "slit") which is described in the following section.

Table 3 summarizes the properties of the image slicer (Older slicers offering lower resolutions are also listed for completeness). The second column lists the number of slices typically present with the respective slicer; column 3 gives the slicer efficiency relative to the high-resolution slicer (see

Table 2: The CES spectral format

| Order # | Wavelength | | | Spectrum length (Å) | Order # | Wavelength | | | Spectrum length (Å) |
|---------|------------|--------|---------|---------------------|---------|------------|---------|--------|---------------------|
| | Min | Blaze | Max | | | Min | Blaze | Max | |
| 65 | 3459.0 | 3479.3 | 3512.9 | 22.9 | 64 | 3513.0 | 3533.7 | 3567.9 | 23.3 |
| 63 | 3568.0 | 3589.8 | 3624.9 | 23.6 | 62 | 3625.0 | 3647.7 | 3682.9 | 24.1 |
| 61 | 3683.0 | 3707.4 | 3741.9 | 24.4 | 60 | 3742.0 | 3769.2 | 3806.9 | 24.8 |
| 59 | 3807.0 | 3833.1 | 3871.9 | 25.3 | 58 | 3872.0 | 3899.2 | 3938.9 | 25.9 |
| 57 | 3939.0 | 3967.6 | 4008.9 | 26.2 | 56 | 4009.0 | 4038.5 | 4080.9 | 26.6 |
| 55 | 4081.0 | 4111.9 | 4154.9 | 27.1 | 54 | 4155.0 | 4188.0 | 4231.9 | 27.5 |
| 53 | 4232.0 | 4267.1 | 4312.9 | 28.1 | 52 | 4313.0 | 4349.1 | 4396.9 | 28.6 |
| 51 | 4397.0 | 4434.4 | 4483.9 | 29.2 | 50 | 4484.0 | 4523.1 | 4572.9 | 29.8 |
| 49 | 4573.0 | 4615.4 | 4666.9 | 30.4 | 48 | 4667.0 | 4711.5 | 4765.9 | 31.0 |
| 47 | 4766.0 | 4811.8 | 4867.9 | 31.7 | 46 | 4868.0 | 4916.4 | 4973.9 | 32.3 |
| 45 | 4974.0 | 5025.7 | 5084.9 | 33.1 | 44 | 5085.0 | 5139.9 | 5201.9 | 33.8 |
| 43 | 5202.0 | 5259.4 | 5324.9 | 34.6 | 42 | 5325.0 | 5384.6 | 5452.9 | 35.5 |
| 41 | 5453.0 | 5516.0 | 5587.9 | 36.2 | 40 | 5588.0 | 5653.9 | 5727.9 | 37.1 |
| 39 | 5728.0 | 5798.8 | 5875.9 | 38.2 | 38 | 5876.0 | 5951.4 | 6031.9 | 39.1 |
| 37 | 6032.0 | 6112.3 | 6195.9 | 40.3 | 36 | 6196.0 | 6282.1 | 6369.9 | 41.4 |
| 35 | 6370.0 | 6461.6 | 6557.9 | 42.6 | 34 | 6558.0 | 6651.6 | 6747.9 | 43.8 |
| 33 | 6748.0 | 6853.2 | 6954.9 | 45.1 | 32 | 6955.0 | 7067.3 | 7173.9 | 46.5 |
| 31 | 7174.0 | 7295.3 | 7407.9 | 48.0 | 30 | 7408.0 | 7538.5 | 7656.9 | 49.6 |
| 29 | 7657.0 | 7798.4 | 7924.9 | 51.3 | 28 | 7925.0 | 8076.9 | 8209.9 | 53.2 |
| 27 | 8210.0 | 8376.1 | 8517.9 | 55.2 | 26 | 8518.0 | 8698.2 | 8849.9 | 57.3 |
| 25 | 8850.0 | 9046.2 | 9208.9 | 59.5 | 24 | 9209.0 | 9423.1 | 9596.9 | 62.0 |
| 23 | 9597.0 | 9832.8 | 10019.9 | 64.7 | 22 | 10020.0 | 10279.7 | — | 67.7 |

Sects. 4.6 and 4.7); column 4 lists the width of the slicer produced equivalent "slit" at the entrance to the spectrograph; the width of the slicer profile on the CCD (perpendicular to the dispersion, see Sect. 4.5) is given in column 5; column 6 gives the achievable resolving power for each slicer; and column 7 lists the line width corresponding to this resolving power at a selected wavelength of 5400 Å (to show an example). Note that this line width is wavelength dependent.

Note also that the number of slices, profile width, achievable resolving power, and line width are given here as ranges reflecting the typical uncertainties encountered during instrument setup. Instrumental setup is a time consuming and delicate procedure and in practice the optimum spectral resolution cannot always be guaranteed. At any rate an attempt is made to achieve resolution values within the listed ranges (see Sect. 7.5).

Table 3: The CES image slicers

| Image slicer | # of slices | Relative slicer efficiency | Equivalent "slit" width | Profile width on CCD | Resolving power | Line FWHM @ 5400 Å |
|--------------|-------------|----------------------------|-------------------------|----------------------|-----------------|--------------------|
| High-res. | 12 | 1.00 | 108 μm | 350-420 pixel | 220,000-235,000 | 2.65-2.83 pixel |
| Medium-res. | 7 | 1.20 | 216 μm | ~245 pixel | 135,000-150,000 | 4.15-4.62 pixel |
| Low-res. | 5 | 1.25 | 341 μm | ~175 pixel | 80,000-100,000 | 6.23-7.79 pixel |

4.5 The image slicer profile

The intensity profile of the spectrum perpendicular to the dispersion direction is shown in Fig. 2. In this figure both the profiles obtained with the flatfield lamp and the profile of a stellar exposure are compared. Small differences are visible; they are further discussed in Sect. 8.

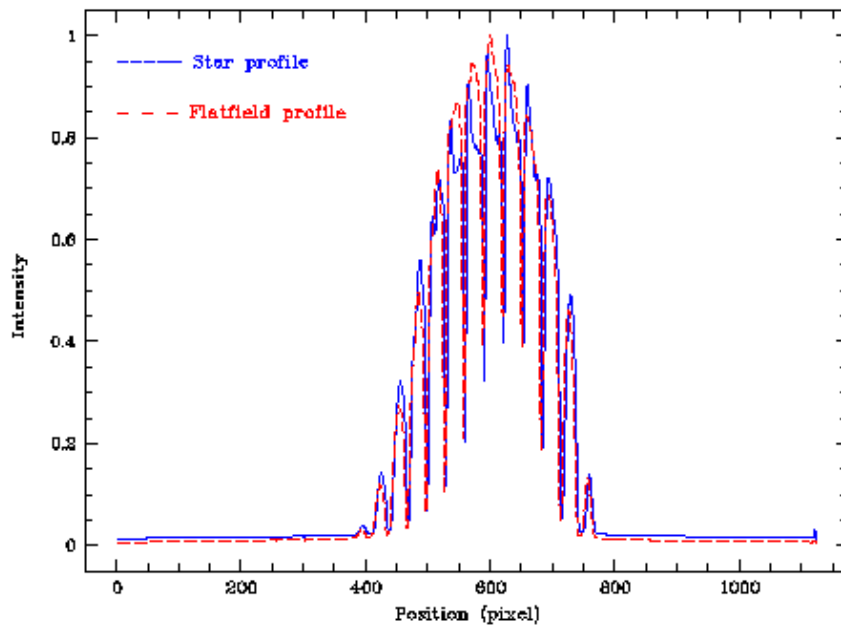


Figure 2: The profile of the image slicer (perpendicular to the dispersion)

4.6 The instrumental efficiency

The "end-to-end throughput" or total efficiency of the CES including the atmosphere (for La Silla mean extinction), the total optical train (fibre, high-res. image slicer, spectrograph optics) as well as the detector was determined for several blaze wavelengths using spectrophotometric standard stars from the following two publications:

- Hamuy M., Walker A.R., Suntzeff N.B., Gigoux P., Heathcote S.R., Phillips M.M., 1992, PASP 104, 533. Southern spectrophotometric standards. I
- Hamuy M., Suntzeff N.B., Heathcote S.R., Walker A.R., Gigoux P., Phillips M.M., 1994, PASP 106, 566. Southern spectrophotometric standards. II.

Since all observations have to be made through the fibre which has a fixed aperture of $2''$ diameter, this type of measurement depends strongly on the seeing conditions. Fig. 3 shows the total efficiency of the CES as a function of wavelength; it is valid for a seeing of $1''$ or better. For greater seeing values the instrumental efficiency decreases.

The thin blue line in Fig. 3 depicts the inferred efficiency accounting for the blaze function of each order (cf. Tab. 2); the thick black line is an interpolation of the efficiency measurements made at various blaze wavelengths and thus an upper envelope to the true efficiencies. Vertical dashed red lines mark wavelengths for which signal-to-noise ratio calculations are presented in the next section (see Fig. 4).

4.7 Signal-to-noise ratios and exposure times

Signal-to-noise ratios achievable for various types of star at a range of selected blaze wavelengths and as a function of exposure time are shown in Fig. 4. The following conditions were assumed for these plots:

- Binning 1x1. Applying binning can improve the signal-to-noise ratio for low count levels. To estimate this one must consider the CCD read-out-noise of 3.4 electrons per unbinned pixel

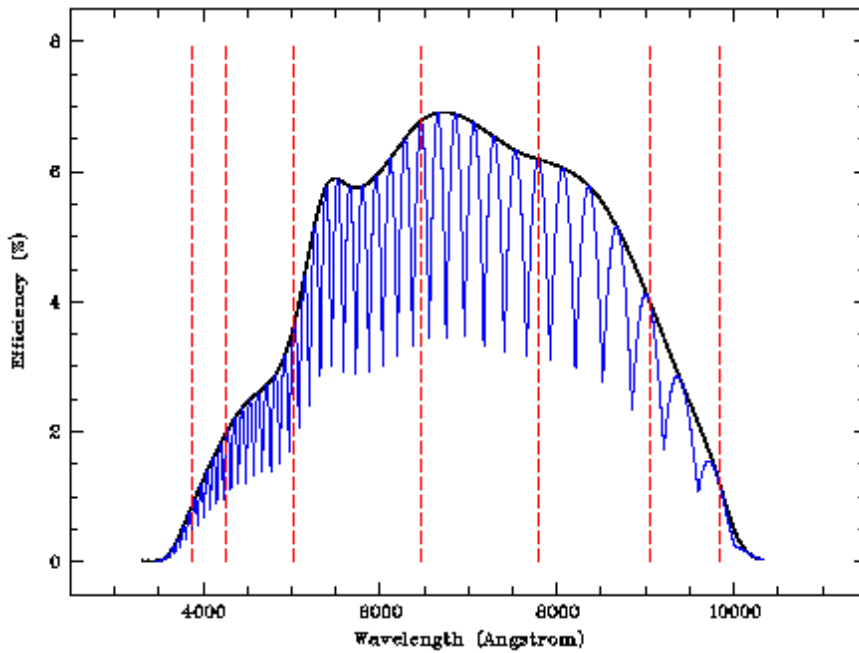


Figure 3: Total efficiency of the CES, including optics and CCD.

(rms) in normal R/O mode (see Sect. 5.3), and take into account the number of image pixels combined into one spectral pixel, i.e. the width of the image slicer profile (see Sect. 4.4 and Tab. 3).

- Observation at blaze wavelengths where the efficiency is maximal. See Fig. 3 for the efficiency variation.
- Seeing $1.0''$. Due to the fixed aperture size of the CES fibre of $2.0''$ on the sky larger seeing values lead to a degradation of the efficiency.
- Observation at airmass 1.0 (minimum extinction).
- La Silla mean extinction values were assumed.

Fig. 4 shows the achievable S/N ratio for exposure times between 1 and 60 min for three different spectral types and two stellar magnitudes. From top to bottom: B2 with $V=6.0$, B2 with $V=9.0$, A0 with $V=6.0$, A0 with $V=9.0$, G0 with $V=6.0$, and G0 with $V=9.0$. As labelled in each panel of the figure, 7 different blaze wavelengths were selected:

- 3833 Å (cyan line)
- 4267 Å (blue line)
- 5026 Å (green line)
- 6462 Å (yellow line)
- 7798 Å (red line)
- 9046 Å (magenta line)
- 9832 Å (black line)

In Fig. 3 the positions of these blaze wavelength are marked by vertical dashed red lines in order to show their location within the total efficiency function.

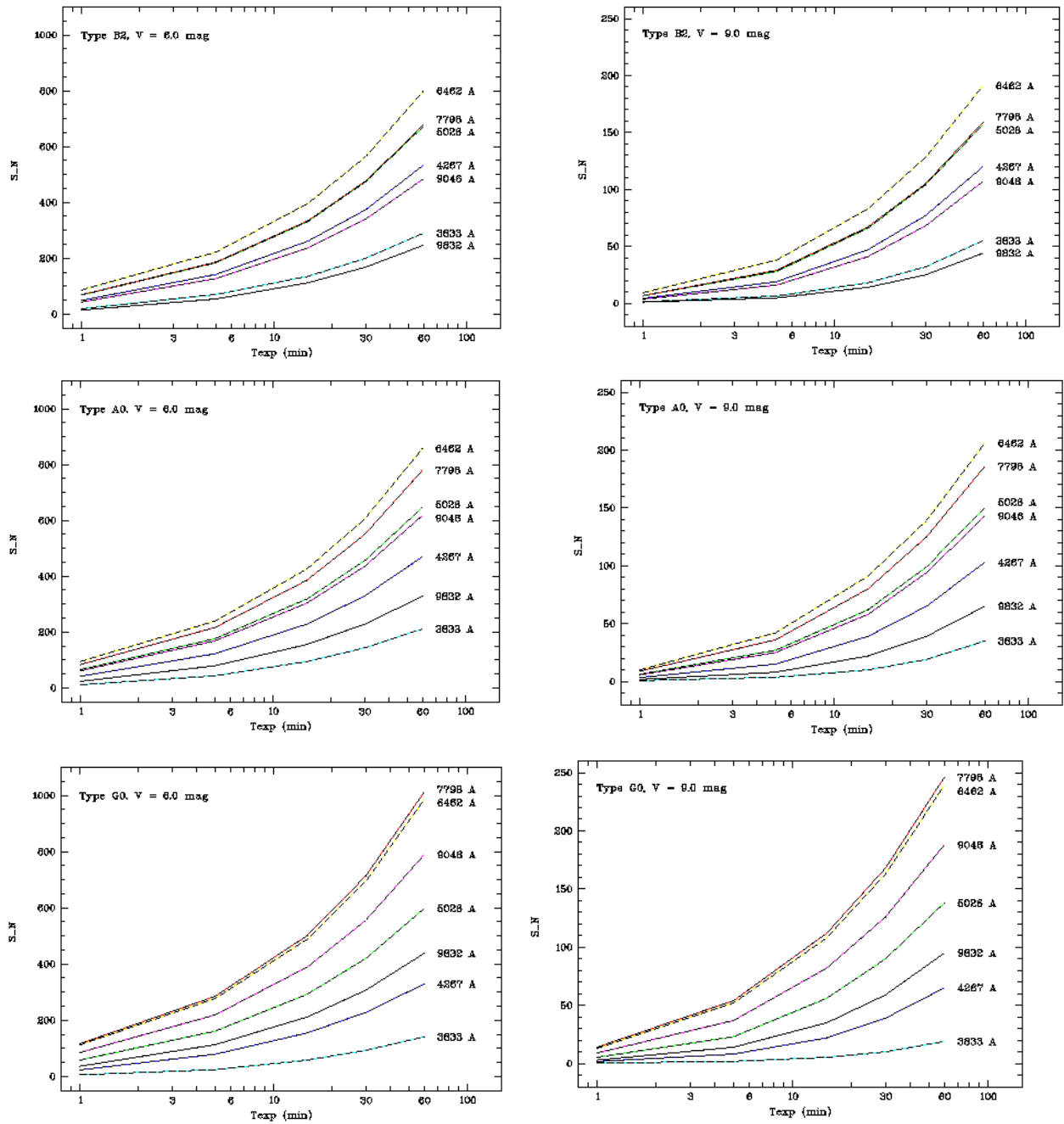


Figure 4: Signal-to-noise ratios as a function of exposure time

4.8 The CES exposure meter

The CES is equipped with an exposure meter (a copy of the UVES exposure meter) which is a photomultiplier that registers light that is blocked by the exit slit of the predisperser. It displays registered count rates and produces a real-time plot of the exposure level (count rate) vs. time. The exposure meter is useful to check any variations of the light entering the instrument which may be due to, e.g.

- clouds,
- changes in atmospheric transmission,
- seeing changes,
- guiding or object centering errors.

It must be noted that the count rates given by the exposure meter are not identical to the count rates that the CCD receives. No absolute calibration is offered for this (proportional) relation, due to the multitude of possible CES instrument settings, but observers can produce their own relative calibration (conversion factor from exposure meter count rates to CCD counts per exposure interval) for their specific setup by comparing exposure meter count rates with counts collected in the science frame. This can be useful to scale exposure times for subsequent exposures.

It should also be noted that currently the exposure meter can only be used for stars that are bright enough and when observing not too far in the blue; e.g. below 4500 Å it gives sufficient counts only for stars brighter than 7 mag, whereas at 5500 Å it can be used for stars up to 9 mag. We plan to extend this range somewhat to fainter stars.

4.9 Instrumental stability

The active control of the CES predisperser and grating provides a very high wavelength stability that has been repeatedly verified. This stability implies that for many scientific programmes it is not necessary to take repeated wavelength calibrations during the night. Whether or not wavelength calibrations should be repeated depends, of course, on the specific requirements of the user for calibration accuracy. To aid this decision the typical variation of the central wavelength on the CCD is illustrated here.

Measured at 5400 Å a variation of only 0.05 pixels rms or 0.2 pixels peak-to-peak is seen in the course of a 10 hour night. This corresponds (at the given wavelength) to a variation in radial velocity units of only 25 m/s rms or 100 m/s peak-to-peak. The first panel of Fig. 5 shows the wavelength drift behaviour in units of CCD pixels (y-coordinate is direction of dispersion) as measured during one night.

Observers should note in any case that La Silla observatory receives weak Earth quakes quite frequently which can occasionally lead to wavelength shifts larger than demonstrated here.

In the direction perpendicular to the dispersion (x-coordinate on the CCD) larger shifts of 1 - 5 pixels have repeatedly been measured. An example is shown in the second panel of Fig. 5. The cause is currently being investigated. These shifts correspond to a non-negligible fraction of the width of individual slices (see Fig. 2 for the slicer profile) with consequences for the performance of flatfielding. See [1] for the latest measurements of these drifts.

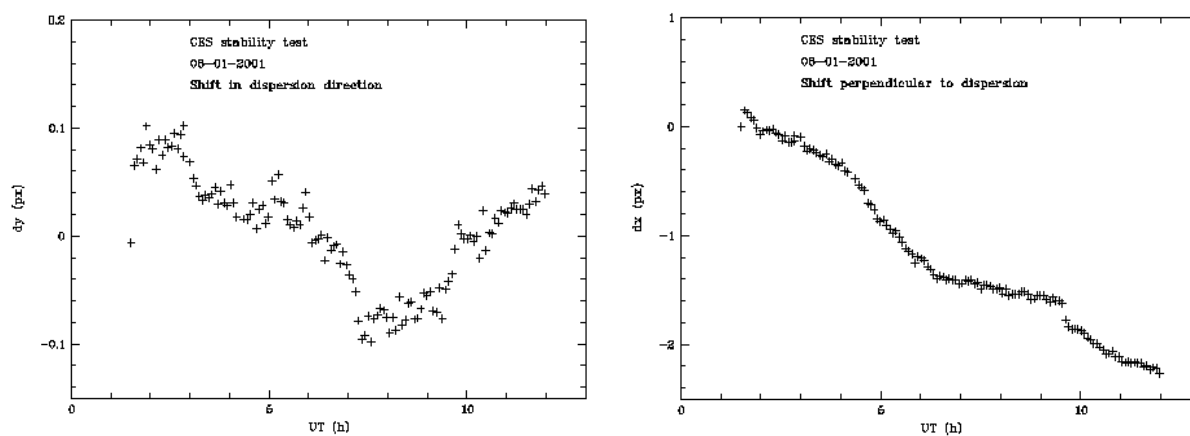


Figure 5: Nightly instrumental stability

5 Detector characteristics

5.1 General description of CCD #61

The CES is used together with ESO CCD #61 which is one of ESO's standard EEV CCDs. It is a monolithic, thinned and back-illuminated chip with 2048x4096 pixels of size $15\ \mu\text{m}$. It has been selected for its very high efficiency in the blue part of the spectrum (below $4000\ \text{\AA}$, see Sect. 5.4 and Fig. 6) in order to compensate for the reduced efficiency of the instrument optics in this regime.

5.2 CCD format

Only the right half of CCD #61 is used and exposed to light from the instrument. It is read out through a single read-out port. The used region of the CCD is 1024x4096 pixels plus 50 pixels each for overscan (first 50 columns) and prescan (last 50 columns) so that the FITS file contains 1124x4096 pixels.

5.3 CCD read-out speeds and binning

Three CCD read-out (R/O) speeds are offered: normal (`normal`, 100 kps), fast (`fast`, 225 kps), and very fast (`vfast`, 625 kps). The only binning modes offered are 1×1 and 4×1 , i.e. no binning in the dispersion direction is offered. Note that "X" is the direction perpendicular and "Y" is the direction parallel to the dispersion (in the CCD image "lambda goes up").

Recommended R/O speed for scientific exposures is `normal`. Programmes which require minimum overhead times (i.e. R/O time, data transfer, and storage) should use `fast` R/O. CCD binning also reduces the overheads. `vfast` R/O is not recommended for scientific applications.

Tab. 4 lists the temporal overheads for the various R/O speed and binning modes. They are precise to ± 1 sec.

Table 4: CCD modes and read-out/transfer time

| Binning XxY | Normal R/O | Fast R/O | Very fast R/O |
|-------------|------------|----------|---------------|
| 1x1 | 51 sec | 26 sec | 15 sec |
| 4x1 | 16 sec | 11 sec | 7 sec |

5.4 CCD quantum efficiency

Fig. 6 shows the quantum efficiency curve of CCD #61. It is shown only for completeness purposes. Note that the CCD constitutes only part of the optical train of the instrument. Observers wishing to know the overall instrument efficiency or to determine exposure times are referred to Sects. 4.6 and 4.7.

5.5 CCD cosmetics

A double bad column (2 pixels wide) is present at $X = 301-302$ which extends over $Y = 211 - 4096$. In the RED path this column is located outside of the recorded spectrum or in or near the extreme faint slice. In the BLUE path the column runs through the recorded spectrum.

As all EEV CCDs also CCD #61 has rows of somewhat changed efficiency at intervals of 512 pixels leading to narrow spikes in the spectrum. However, this effect flatfields out very well.

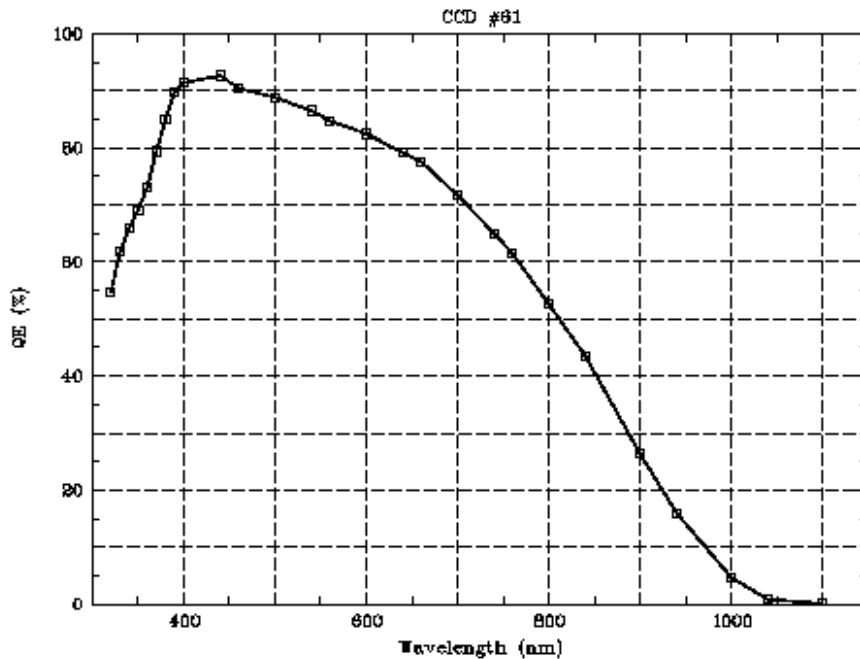


Figure 6: Quantum efficiency curve of CCD #61

5.6 Cosmic ray hit rate

The typical cosmic ray hit rate is $5 \cdot 10^{-5} \pm 10^{-5}$ hits per hour per unbinned image pixel, i.e. about 0.020 hits per hour per spectral pixel. Thus in the complete spectrum (4096 pixels) about 82 hits must be expected in a one hour exposure (see Sect. 8.6 for suggestions for the treatment of cosmics).

5.7 Detector monitoring

Several parameters of the CCD are monitored at regular intervals for a number of selected read-out modes. These parameters are

- Bias
- Conversion factor
- Read-out noise
- Shutter delay
- Maximum non-linearity

The monitored read-out modes are

- Normal R/O, binning 1x1
- Normal R/O, binning 4x1
- Fast R/O, binning 1x1
- Fast R/O, binning 4x1
- Very fast R/O, binning 1x1

- Very fast R/O, binning 4x1

The results can be found via the CES web pages [1]. Results of dark current measurements can also be found via this page.

6 The CES observing templates

Observations with the CES are carried out under the VLT standard which implies the preparation of observing blocks (OBs) with the p2pp tool. See Sect. 2 and [2].

An OB is the observational unit to be carried out at any time. An OB contains a selection of one or more so-called templates which are predefined tasks for which usually a number of parameters can be set by the user. Three types of templates exist:

- Calibration templates,
- Observation templates,
- Acquisition templates.

The templates available for the CES are described in the following Sections. They are also summarized in Table 4 which also lists the selectable parameters for each template.

Observers should note that only the listed parameters are selectable, and that every parameter selection is a pre-selection. When an observing template is running, none of these parameters can be changed. E.g. it is not possible to change the exposure time while an exposure is running. Changes of exposure time, or stopping an exposure is only possible via the OS (observation software) panel which is exclusively operated by the operator. Any such change will only be made exceptionally by the operator (e.g. when clouds force to stop an exposure); observers should as far as possible avoid the need for such changes.

6.1 Genuine Calibration templates

The following templates are available for the calibration of CES data:

CES_hcfa_cal_thAr This calibration template is for wavelength calibration through the CES fibre. It uses the HCU to make an exposure with a ThAr hollow cathode lamp. Typical exposure times are 30 - 60 sec for binning 1x1 and the high-resolution slicer. Usually, the best exposure time for a given wavelength region, image slicer, and CCD binning is determined in the afternoon from test exposures.

CES_hcfa_cal_flats This calibration template is for flatfielding through the CES fibre using the flatfield lamp of the HCU. Typical exposure times are of the order 15 sec, but depend on the central wavelength, chosen image slicer, and CCD binning.

CES_hcfa_cal_darks This calibration template is for bias or dark exposures, i.e. any exposure with the CCD shutter closed.

CES_hcfa_cal_back This calibration template can be used to determine the level of parasitic light in the instrument, inserting the dust cover of the HCFA into the light path in order to avoid light contamination (during daytime) from the dome.

In all of these calibration templates users can specify the same parameters, i.e. exposure time, CCD R/O speed, CCD binning, and number of exposures.

6.2 Special Calibration template for wavelength setting

Due to the very stable behaviour of the CES in terms of retaining the selected central wavelength a special strategy has been devised for wavelength setting or change. This is done via a special template of the calibration type:

CES_hcfa_cal_setwave This template moves predisperser prism and grating near the correct position for the chosen central wavelength, and then starts an interactive dialog permitting the operator to center the predisperser and grating precisely on the desired position. For the predisperser this is done via flatfield exposures vignetted by the exit slit of the predisperser unit put to its minimum width, whereas for the grating it is done using regular ThAr exposures.

The reason for doing wavelength changes only with this special template lies in the active control of predisperser and grating. `CES_hcfa_cal_setwave` is the only template that permits to select the central wavelength. Once the correct central wavelength is set, no other template can change it.

`CES_hcfa_cal_setwave` is also the only template that provides the software with the information on which image slicer is used by providing the width of the effective entrance slit produced by the image slicer (see Table 2, third column). The software uses this value to calculate the correct width of the predisperser exit slit for the chosen central wavelength. Note that there is no software control of the image slicer selection itself which is done manually.

Apart from the mentioned parameters, central wavelength and entrance width, the other parameters that can be chosen for this template are CCD R/O speed, CCD binning, and exposure time; the exposure time is usually modified by the operator during the dialog to adapt to the appropriate exposure levels for the (vignetted) flatfield or the ThAr exposures.

6.3 Science template

For science exposures only one CES template exists:

CES_hcfa_obs_all This template is for science exposures of a user-selected target. Contrary to the calibration templates described above, an OB which contains this science template requires a preceding acquisition template in order to move the telescope (see Sect. 6.4); The OB must also contain the coordinates of the target.

The parameters that can be selected for `CES_hcfa_obs_all` are exposure time, CCD R/O speed, CCD binning, number of exposures, and the “Standard Star” flag.

The Standard Star flag is set to `SCIENCE` by default, but can also be set to `STANDARD`. This will have two consequences:

1. The exposure will be treated as a calibration frame and included among the calibrations of *every* program data-package of the night regardless of the Program-ID.
2. There will be *no* proprietary period for the `STANDARD` exposures, i.e. they can be freely requested from the ESO archive.

6.4 Acquisition template

Only one acquisition template exists:

Table 5: The CES observing templates

| Template | Type | Selectable Parameters | Defaults |
|----------------------|-------------|--|--|
| CES_hcfa_acq | Acquisition | None | None |
| CES_hcfa_obs_all | Science | Exposure time (s) CCD R/O speed (n=8, f=10, vf=9) CCD X binning CCD Y binning Number of exposures Standard Star flag | NODEFAULT 8 1 1 1 SCIENCE |
| CES_hcfa_cal_darks | Calibration | Exposure time (s) CCD R/O speed (n=8, f=10, vf=9) CCD X binning CCD Y binning Number of exposures | NODEFAULT 8 1 1 3 |
| CES_hcfa_cal_back | Calibration | Exposure time (s) CCD R/O speed (n=8, f=10, vf=9) CCD X binning CCD Y binning Number of exposures | NODEFAULT 8 1 1 3 |
| CES_hcfa_cal_flats | Calibration | Exposure time (s) CCD R/O speed (n=8, f=10, vf=9) CCD X binning CCD Y binning Number of exposures | NODEFAULT 8 1 1 1 |
| CES_hcfa_cal_thAr | Calibration | Exposure time (s) CCD R/O speed (n=8, f=10, vf=9) CCD X binning CCD Y binning Number of exposures | NODEFAULT 8 1 1 1 |
| CES_hcfa_cal_setwave | Calibration | Center Wavelength (nm) Entrance width (0.108, 0.216, 0.341) Exposure time (s) CCD R/O speed (n=8, f=10, vf=9) CCD X binning CCD Y binning | NODEFAULT NODEFAULT NODEFAULT 8 4 1 |

CES_hcfa_acq This template moves the telescope to the coordinates specified for the target in the OB. The telescope operator then centers the object in the fibre (see Sect. 3.1) and starts autoguiding (see Sect. 3.2). No parameters are selectable with this template.

In the situation that the observer does not want to make another preset, because s/he wants to continue on the same target which is already centered in the fibre, s/he must inform the operator that the acquisition template should be skipped.

7 Characteristics of instrument setup delivered to the observer

7.1 Alignment of the spectrum with CCD columns

During instrument setup the instrument team will align the spectrum with the CCD columns to better than 1 pixel over the full length of 4096 pixels.

7.2 Spectral line tilt

The tilt of the spectral lines (non-parallelity with respect to the CCD rows) will typically be adjusted to be less than 0.1 pixels in 100 pixels. This adjustment can only be made at one wavelength setting as line tilt depends slightly on wavelength. If more than one wavelength is to be used, a compromise must be found. Observers should communicate the wavelength at which the setup is to be made. Note that any such setup adjustments are time consuming and therefore only possible during daytime. As mentioned in Sect. 4.2 changes of instrument path introduce strong line tilt; they are not regularly supported at night time.

7.3 Variation of the width of spectral lines along the slicer profile

Variations of the width of spectral lines from one side of the spectrum to the other (at constant wavelength) will typically be adjusted to be less than 0.1 pixels in 100 pixels. As for the line tilt (Sect. 7.2) the variation of the line width will only be optimized at one wavelength.

7.4 Instrument focus

During setup the instrument focus will be optimized for the chosen wavelength to yield the optimum resolving power. As for line tilt (Sect. 7.2) and line width variation (Sect. 7.3) the focus optimization can only be prepared at one selected wavelength.

7.5 Spectral line width and resolving power

Optimization of line tilt, line width variation, and instrument focus will ensure a minimum line width and hence a maximum resolving power. Currently achievable typical resolving power values are summarized in Table 3 which also lists the typically obtained line width for a wavelength of 5400 Å (as an example).

7.6 Presence and location of ghost features

The chosen wavelength region will be checked for the presence of ghost features. These are unavoidable reflections produced by the Echelle grating and appear as emission-type features. Should a ghost feature fall onto a spectral region of importance for the observing program the observer can decide to make a small change of the central wavelength in order to free the needed spectral region from the ghost feature (see strategy outlined in Sect. 8.5). Wavelength change is done with the template `CES_hcfa_cal.setwave` (see Sect. 6.2).

Note that such changes of the central wavelength by a few Å do not affect the previously listed properties of the setup.

8 Instrument features to be considered for proper data analysis

8.1 Bias instability

The high read-out performance of the standard ESO FIERA CCD controller used for the CES CCD leads to a variation of the bias level of the order 1 ADU. As the extraction of a CES spectrum requires the summation over several hundred pixels the resulting uncertainty of the bias level in the extracted spectrum is of the order several hundred ADU. A correction strategy is therefore mandatory.

The bias variation depends on the activity of the controller and is not predictable in a straightforward manner. However, the overscan of the CCD (first 50 columns; see Sect. 5.2) can be used for a correction in the following way:

- Compare the mean value in the overscan of the bias frame with the mean value of the overscan of the frame to be bias subtracted (flatfield or science exposure). It is recommended to use only the first 20 columns of the overscan (i.e. the first 20 columns of the image) for this correction as there may be some light contamination on the subsequent columns.
- Add the difference to the bias frame such that the overscans of bias frame and frame to be reduced have the same mean value.
- Then subtract the modified bias frame from the frame to be reduced.

8.2 Dark current

As several hundred CCD image pixels are summed up into one spectral pixel for the extraction of the spectrum, the correction of the dark current of the CCD is important for long exposures. Typical dark current values are about 2.4 e/px/hr (unbinned CCD, normal R/O).

Dark current measurements for CCD #61 can be found via the CES web pages [1]. They should be used as an indicative only. It is recommended that observers use the dark calibration frames provided with the SCS (see Sect. 3.4).

When correcting for the dark current the dark exposure must first be bias subtracted with the procedure outlined in Sect. 8.1, i.e. correcting the bias instability by comparing the overscan regions of the CCD. The bias subtracted dark current measurement must then be scaled to the exposure time of the frame to be reduced before subtracting it from this frame.

8.3 Parasitic light

Observers of faint objects and with long exposure times may want to determine the level of parasitic light present in the instrument. This is done via background exposures with the template CES_hcfa_cal_back (see Sect. 6.1).

In data reduction the treatment of the parasitic light level is identical to the treatment of the dark current. The background exposure replaces the dark exposure in the reduction.

8.4 Flatfielding performance

Special care must be taken in order to use an appropriate flatfielding strategy. As flatfielding is done through the fibre and image slicer flatfield exposures have the full slicer profile (see Fig. 2); hence they are not "flat", but highly structured.

A plain division of the science frame by the flatfield frame is prohibitive as it leads at the flux minima between the slices to a division of small numbers by small numbers; it thus gives CCD columns of little flux unduely high weight.

Also, the instrumental drift in the direction perpendicular to the dispersion direction (see Fig. 5, second panel) can lead to non-negligible shifts between flatfield and science exposures which can only be minimized, if repeated flatfield exposures are taken during the night. However, this implies substantial temporal overheads.

In order to perform appropriate flatfielding, the flatfield exposure(s) must first be "flattened", i.e. normalized. An easy way to do this is to average all CCD rows in order to obtain the average flatfield profile which is then converted into a two-dimensional image each row of which consists of this profile. Subsequent division of the original flatfield by this two-dimensional "profile image" yields the normalized flatfield. However, any remaining alignment imperfection (see Sect. 7.1), even at the subpixel level, leads to the fact that the average profile does not precisely represent the profile at all CCD rows, and residual structure in the normalized flatfield is seen, especially near the bottom and top of the CCD frame.

A better flatfield normalization is obtained by fitting each column of the flatfield frame with a low-order polynomial, and dividing this column by the obtained fit. Caution must be taken when using this method, if ghost features are present which should be excluded from the region over which the polynomial fit is performed. This strategy ensures that all pixels in the normalized flatfield are of order unity, and dividing the science frame by this normalized flatfield removes well the pixel-to-pixel variations of the CCD.

Another flatfielding strategy often proposed for fibre-fed spectrographs shall be mentioned here. It consists of first extraction the science frame and the flatfield frame to one-dimensional spectra which are then divided. Due to the differences seen for the CES in the profiles from a star and from a flatfield (see Fig. 2), this method leads to results which are not as good as the normalization strategies described above.

8.5 Ghost features

Ghost features are reflections produced by the Echelle grating that occur in about 50% of the CES wavelength settings. They appear as emission-type features. The best of the flatfielding strategies described in Sect. 8.4 succeeds in many cases in obtaining a good removal of the ghost feature from the science frame, but with a substantial degradation of the S/N ratio of the extracted spectrum at the position of the ghost feature.

Observers should always check their wavelength region for the presence of ghost features (see also Sect. 7.6) and whether they fall at the position of a spectral line of interest. If this is so, then the ghost feature can be moved by changing the central wavelength by about 1 - 2 Å. This will move the interesting spectral line to another position on the CCD. The ghost feature usually follows this movement, but at a smaller rate. This adjustment of the central wavelength can be done in the afternoon using template CES_hcfa_cal_setwave. Of course, care must be taken that the wavelength change does not cause the loss of any other important spectral features near the end of the covered spectral range. Finding the best compromise for the central wavelength is usually an iterative process.

8.6 Treatment of cosmic rays

Due to the summation of several hundred of image pixels into one spectral pixel, and given the present cosmic ray hit rate, the number of accumulated cosmic rays in a spectrum is quite substantial (see Sect. 5.6).

Many strategies for the removal of cosmic rays exist. Because of the highly structured profile of the spectrum produced by the image slicer (see Fig. 2) the performance of filtering methods performed on the image or on the extracted spectrum is very limited.

At least for longer exposures (over 10 min) we recommend a more robust (but also more computationally intensive) strategy that consists of splitting the exposure into a set of three exposures (each of which with a third of the required exposure time). The resulting three two-dimensional frames are then normalized to the same flux level (after bias and dark/background subtraction), and compared pixel by pixel to find cosmic rays. Any pixel that deviates by more than a selectable threshold (depending on the S/N ratio) from the median value of the (normalized) fluxes of the same pixel in the three frames is then identified as a cosmic ray and replaced by that median value. After this modification the three frames can be de-normalized and added.

Splitting the exposure into three implies that three times the R/O noise is accumulated. This should be considered in a decision for or against this strategy.

8.7 Straylight pedestal

A considerable amount (few percent) of diffuse light is seen beneath the light pattern of the image slicer (see Figure 2). This effect is produced by the image slicer itself. The light distribution is only slightly non-uniform along the dispersion direction, representing a low-resolution version of the stellar spectrum. For practical purposes it can usually be treated as if it were uniform.

If not corrected for, this effect leads to the underestimation of the equivalent widths of spectral lines. Special care must be taken by observers interested in line strengths.

In most cases, the amount of diffuse light present cannot be directly measured, and differences were found for various types of input light beams (e.g. extended vs. point sources such as flatfield vs. star). In principle there are two types of possibilities to correct for this effect:

1. Comparison with a solar spectrum A solar spectrum can be taken as a reference with the CES either on the day-sky, on the Moon, on one of Jupiter's moons (Ganymede or Europa), or on a bright asteroid. Then this spectrum can be compared with a solar atlas, e.g. an FTS spectrum such as given in

- Kurucz et al. 1984, NSO Atlas No. 1, Solar Flux Atlas from 296 to 1300 nm.

The recorded equivalent widths can then be compared with those obtained from the solar atlas and a wavelength dependent measurement of the strength of the diffuse light effect can be obtained for the purpose of applying a correction to line equivalent widths measured in stellar spectra. A solar spectrum is taken every afternoon and provided as part of the SCS (see Sect. 3.4).

2. Taking spectra of stars with saturated lines At certain wavelengths such as the NaI D region (589.0 nm and 589.6) stars can be found which have saturated interstellar lines; other wavelength regions have totally opaque telluric lines, (e.g. oxygen lines near 763.5 nm or water vapour lines in the region 930 nm and 957 nm, the latter being variable, best observed at high airmass). In such cases the amount of scattered light can be directly measured by determining the minimum flux seen in the saturated lines using rapidly rotating B-stars (few stellar features).

Observers of the NaI D region can find suitable early-type stars with saturated interstellar NaI D lines in the following paper:

- Welty D.E., Hobbs L.M., Kulkarni V.P.: 1994, ApJ 436, 152.

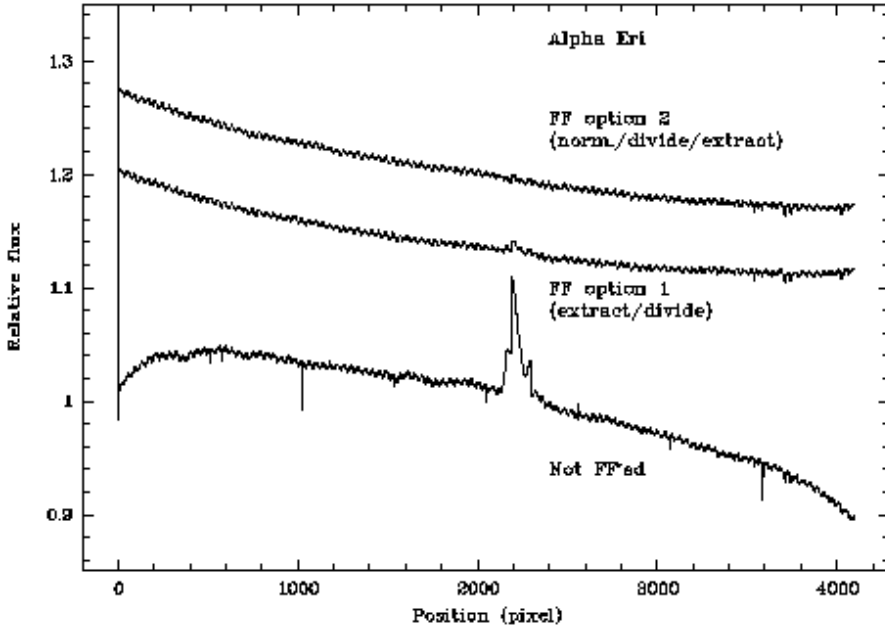


Figure 7: Instrumental features: ghost, spikes, ripple, and flatfielding performance

It is evident that for the majority of wavelength settings only the solar spectrum comparison will be possible.

8.8 Interference pattern seen in continuum

A regular sinusoidal pattern ("ripple") visible in the continuum was discovered by the CES observer G. Mulas who provided us with a detailed report on the subject including a possibility to remove this structure. Subsequent observations have repeatedly revealed the pattern.

The presence of this pattern typically limits the achievable signal-to-noise ratio to about 500. Observing programs aiming at higher S/N ratios must consider this effect.

For stars with relatively low line density it is possible to Fourier analyse this pattern and remove it. This is done using the following formula:

$$F(\lambda) = F_0(\lambda) (1 + 2a \cos(2\pi x/\lambda + d)) \quad (1)$$

where $F_0(\lambda)$ is the spectrum without the ripple, $F(\lambda)$ is the spectrum with the ripple, and λ is the wavelength; the parameters x (ripple frequency in wavelength space), d (ripple phase), and a (ripple amplitude) are to be determined by fitting the above function to the spectrum. This fit is to be done to individual spectra, because the ripple amplitude a can vary from exposure to exposure; the ripple phase d and frequency x are found to be constant for a given wavelength setting. The ripple amplitude is typically higher at good seeing and low airmass.

Differences are also seen between the appearance of the ripple in flatfield exposures and stellar spectra which therefore need to be treated independently.

8.9 An example showing several instrumental features

A demonstration of several of the mentioned instrumental features can be found in Fig. 7. It shows the spectrum of the bright rapidly rotating B-star alpha Eri at a central wavelength of 5395 Å. In

this wavelength region this star has no spectral features of its own and thus serves as a continuum source.

The lower curve is the extracted spectrum without flatfielding. It shows a ghost feature centered on pixel 2200 (cf. Sects. 7.6 and 8.5). Also seen is the interference pattern (described in Sect. 8.8) as a ripple with a period of about 40 pixels. In addition a number of sharp spikes are seen separated by 512 pixels which are detector imperfections (see Sect. 5.5).

The other two curves (shifted upwards for display purposes) show versions of this spectrum after flatfielding with two different methods (cf. Sect. 8.4). The middle spectrum corresponds to the often used method for fibre-fed spectrographs to first extract the spectrum of star and flatfield and then divide. This efficiently removes the spikes, but a residual of the ghost feature is seen. The upper spectrum was produced by dividing the star frame with a flatfield normalized by its mean profile and subsequent extraction of the result. The correction of the ghost feature is much better with this method.

None of the shown flatfield methods can remove the interference pattern, which has a different amplitude and shape in the flatfield and the star exposure. As mentioned in Sect. 8.8, the removal of this pattern must be done in star and flatfield independently and precede the flatfielding process.

---oOo---